

[CASE REPORT]

Myoclonic Epilepsy with Ragged-red Fibers with Intranuclear Inclusions

Tomoya Kawazoe¹, Shinsuke Tobisawa¹, Keizo Sugaya¹, Akinori Uruha^{1,2},
Kazuhito Miyamoto¹, Takashi Komori³, Yu-ichi Goto^{4,5}, Ichizo Nishino^{5,6},
Hiroshi Yoshihashi⁷, Takeshi Mizuguchi⁸, Naomichi Matsumoto⁸, Naohiro Egawa⁹,
Akihiro Kawata¹ and Eiji Isozaki¹

Abstract:

We herein report a case of myoclonic epilepsy with ragged-red fibers (MERRF) harboring a novel variant in mitochondrial cysteine transfer RNA (*MT-TC*). A 68-year-old woman presented with progressive myoclonic epilepsy with optic atrophy and peripheral neuropathy. A skin biopsy revealed p62-positive intranuclear inclusions. No mutations were found in the causative genes for diseases known to be related to intranuclear inclusions; however, a novel variant in *MT-TC* was found. The association between intranuclear inclusions and this newly identified MERRF-associated variant is unclear; however, the rare complication of intranuclear inclusions in a patient with typical MERRF symptoms should be noted for future studies.

Key words: mitochondrial diseases, epilepsies, myoclonic, optic atrophy, peripheral neuropathies, intranuclear inclusions

(Intern Med 61: 547-552, 2022)

(DOI: 10.2169/internalmedicine.7767-21)

Introduction

In myoclonic epilepsy with ragged-red fibers (MERRF), heteroplasmic variants in the mitochondrial tRNA^{Lys} gene account for >90% of the pathogenic variants; m.8344A>G is the most common (>80%), followed by m.8356T>C, m.8363G>A, and m.8361G>A. Other rare pathogenic MERRF variants include m.611G>A in *MT-TF* (mitochondrially encoded tRNA^{Phe}), m.3243A>G in *MT-TLI* (tRNA^{Leu}), m.4279A>G and m.4284G>A in *MT-TI* (tRNA^{Ile}), and m.15967G>A in *MT-TP* (tRNA^{Pro}) (1). To date, there are only a limited number of reports on mitochondrially encoded tRNA^{Cys} (*MT-TC*). A heteroplasmic m.5814 variant was reported as the cause of mitochondrial diseases in three

unrelated patients (2-4). In addition, the m.5814 variant in a homoplasmic state was described in a patient with severe mitochondrial encephalopathy (5).

We herein report a patient with MERRF carrying a novel homoplasmic m.5820C>A variant in the tRNA^{Cys} gene.

Case Report

A 68-year-old Japanese woman presented with a 58-year history of progressive myoclonic epilepsy with optic atrophy and peripheral neuropathy. The patient had no evident family history of similar symptoms, although her maternal grandmother died at a young age for an unknown reason. At 10 years old, the patient developed self-induced pattern-sensitive epilepsy and had photosensitive seizures. Owing to

¹Department of Neurology, Tokyo Metropolitan Neurological Hospital (TMNH), Japan, ²Department of Neuropathology, Charité - Universitätsmedizin Berlin, Germany, ³Department of Laboratory Medicine and Pathology (Neuropathology), TMNH, Japan, ⁴Department of Mental Retardation and Birth Defect Research, National Institute of Neuroscience, National Center of Neurology and Psychiatry (NCNP), Japan, ⁵Medical Genome Center, NCNP, Japan, ⁶Department of Neuromuscular Research, National Institute of Neuroscience, NCNP, Japan, ⁷Department of Clinical Genetics, Tokyo Metropolitan Children's Medical Center, Japan, ⁸Department of Human Genetics, Yokohama City University Graduate School of Medicine, Japan and ⁹Department of Neurology, Kyoto University Graduate School of Medicine, Japan

Received: April 15, 2021; Accepted: July 5, 2021; Advance Publication by J-STAGE: August 24, 2021

Correspondence to Dr. Tomoya Kawazoe, tomoya_kawazoe@tmhp.jp

myoclonic jerks induced by the shape of a cockscomb, sunlight, and television, she constantly wore sunglasses. By 20 years old, mild intellectual disability and action myoclonus of the upper limbs were apparent. She was prescribed clonazepam and phenytoin 10 years later, which relieved the generalized tonic-clonic seizures, but not the myoclonic jerks. The action myoclonus progressed to her lower limbs at 50 years old, making her unable to go outside without assistance by 55 years old. Visual disturbances appeared at approximately the same time. When she was 66 years old, she developed numbness in her distal lower limbs. A neurological examination in our hospital at 68 years old revealed mild intellectual disability, according to the Wechsler Adult Intel-

ligence Scale-Fourth Edition (6), with a mean of 100 and a standard deviation of -2.2 to -1.7; index scores of verbal comprehension, 75; perceptual reasoning, 69; and working memory, 67. This mild intellectual disability was not expected to be progressive, based on her history, at least during the last 48 years. Furthermore, this neurological examination also indicated slurred speech, optic atrophy, hypotonia, myoclonus, mild muscle weakness and atrophy in the distal limbs, decreased tendon reflexes, sensory disturbances, limb ataxia, and constipation. Ptosis, ophthalmoplegia, deafness, and lipoma were not observed. She also showed no progressive dementia, parkinsonism, or evident autonomic dysfunction (except for constipation, which could be considered age-related, based on its severity). Myoclonic hyperkinesia made it difficult for her to walk, sit, or stand still.

Laboratory examinations revealed neither diabetes nor increased serum creatine kinase levels. Lactate and pyruvate levels in the cerebrospinal fluid were mildly elevated [19 mg/dL (normal: 4.2-17.0 mg/dL) and 1.2 mg/dL (normal: 0.3-0.9 mg/dL), respectively]. The respiratory function was normal, and there was no evidence of cardiomyopathy. An electroencephalogram confirmed photosensitivity. The somatosensory-evoked potentials were markedly enlarged, with an amplitude of 90 μ V (normal <10 μ V). A nerve conduction study revealed a sensory neuropathy pattern (Table 1), while electromyography showed myogenic alterations in the distal lower limbs. Brain magnetic resonance imaging revealed cranial bone hypertrophy and mild cerebellar atrophy (Fig. 1A), with slight hyperintensities of the dentate nucleus (Fig. 1B). Cranial bone hypertrophy and mild cerebellar atrophy can be caused by chronic antiepileptic drugs (AED). However, since findings suggesting dentate degeneration are not usually observed in epilepsy patients with chronic AED use, thickening of the skull and a small cerebellum may have been a natural finding in the patient. No other hyperintensities suggesting specific diseases were observed on T2 fluid-attenuated inversion recovery images (Fig. 1C).

Table 1. Nerve Conduction Study Findings.

Nerve	Variable	Patient		Control*	SD
		59 years	68 years		
Median	MCV (m/s)	51.9	56.3	57.7	4.9
	DL (ms)	4.90	3.40	3.49	0.34
	CMAP (mV)	7.8	5.1	7.0	3.0
	SCV (m/s)	42.4	52.2	56.2	5.8
	SNAP (μ V)	9.3	5.4	38.5	15.6
Ulnar	MCV (m/s)	56.9	52.3	58.7	5.1
	DL (ms)	3.90	3.10	2.59	0.39
	CMAP (mV)	11.2	7.8	5.7	2.0
	SCV (m/s)	40.6	31.8	54.8	5.3
	SNAP (μ V)	7.2	4.5	35.0	14.7
Tibial	MCV (m/s)	42.8	41.6	48.5	3.6
	DL (ms)	3.85	3.60	3.96	1.00
	CMAP (mV)	15.3	10.2	5.8	1.9
Sural	SCV (m/s)	NE	NE	51.1	5.9
	SNAP (μ V)	NE	NE	17.2	6.7

CMAP: compound muscle action potential, DL: distal latency, MCV: motor conduction velocity, NE: not elicited, SD: standard deviation, SCV: sensory conduction velocity, SNAP: sensory nerve action potential. *The control values are taken from the third edition of the textbook by Jun Kimura (Electrodiagnosis in diseases of nerve and muscle: principles and practice, Oxford University Press). Mean values are presented.

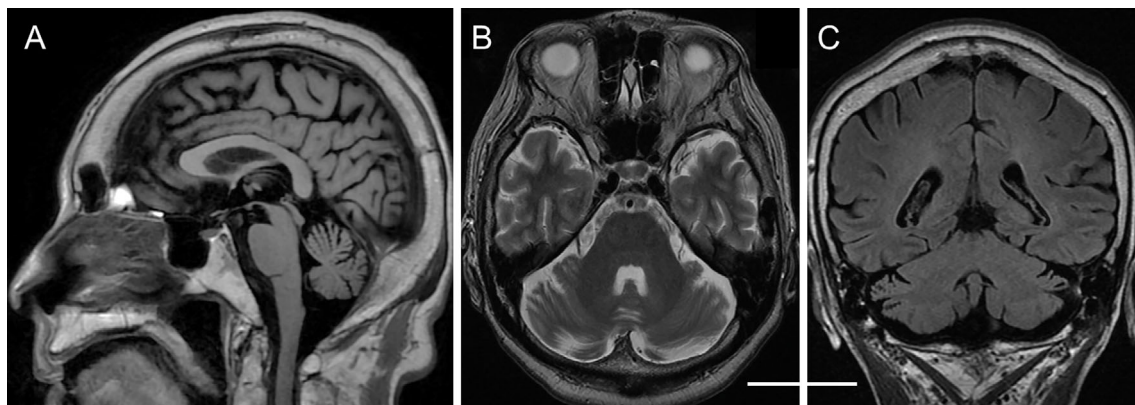


Figure 1. Radiological findings. (A) Sagittal view of a brain MRI T1-weighted image, highlighting cranial bone hypertrophy and mild cerebellar atrophy. (B, C) Axial view of a T2-weighted image (B), and coronal view of a T2-weighted fluid-attenuated inversion recovery image. No specific hyperintensities are observed, except for slight hyperintensities of the dentate nucleus. Scale bar: 5 cm (A-C).

A histological examination of a sural nerve biopsy and a muscle biopsy revealed diffusely reduced myelinated fibers (Fig. 2) and focal cytochrome c oxidase (COX)-deficiency (Fig. 3A), respectively. Electron microscopy showed a marked proliferation of abnormally elongated mitochondria in the subsarcolemmal area (Fig. 3B). To exclude Lafora disease, we simultaneously performed a skin biopsy. No Lafora periodic acid-Schiff inclusion bodies were observed. However, an immunohistochemical analysis of the skin biopsy, using a primary antibody for anti-p62/SQSTM1 (C-terminus) (GP62-C, 1:1000; PROGEN Biotechnik GmbH, Maaßstraße 30, 69123 Heidelberg, Germany), revealed p62-positive intranuclear inclusions (Fig. 4).

A mitochondrial DNA analysis identified a novel variant. Mitochondrial DNA was extracted from the skeletal muscle and blood, amplified via the long and accurate polymerase chain reaction method, and directly sequenced, as previously described (7). A homoplasmic variant (m.5820C>A) of the tRNA^{Cys} gene was identified (Table 2). This variant is not listed in the MITOMAP (“mtDNA coding region & RNA sequence variants” and “mtDNA control region sequence

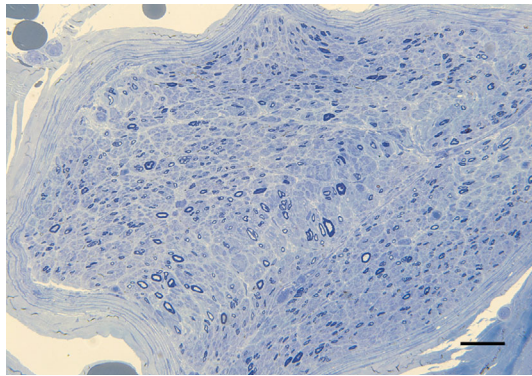


Figure 2. A histological examination of a sural nerve biopsy. Epon-embedded semi-thin section stained with Toluidine blue shows diffusely reduced myelinated fibers. Scale bar: 50 μ m.

variants”) database of genomic variants (8). All other identified variants in Table 2 are present in this database as benign polymorphisms. The enzymatic activities of mitochondrial respiratory complexes I-V and citrate synthase were measured in the mitochondrial fraction of the patient’s skeletal muscle and are expressed as the time-dependent spectrum alterations. Complexes I-IV and citrate synthase were assayed as described previously (9). Complex V was assayed according to the method described by Morava et al. (10). The enzymatic activity of mitochondrial respiratory chain complex IV in the extract was 55% and 69% of the control value when normalized to complex II and citrate synthase activities, respectively (Table 3).

Since intranuclear inclusions were present, we considered the possibility of comorbid neuronal intranuclear inclusion disease. However, GGC-repeat expansions in the *NOTCH2 NLC* gene were not found on repeat-primed polymerase chain reaction. Genetic tests showed no mutations indicative of the following conditions: spinocerebellar ataxia type 1, 2, 3, 6, 7, 8, and 12; dentatorubral-pallidolusian atrophy; fragile X-associated tremor/ataxia syndrome (FXTAS) (30 CGG repeats, normal <45); and Unverricht-Lundborg disease. Whole-exome sequencing identified no disease-causing variants of other nuclear genes.

Discussion

The present patient was clinically diagnosed with MERRF based on its four canonical features: myoclonus, generalized epilepsy, ataxia, and the appearance of ragged-red fibers in the muscles. The presence of myopathy, peripheral neuropathy, and optic atrophy was also consistent with MERRF. After the MERRF diagnosis, we adjusted the antiepileptic drugs (phenytoin and carbamazepine were discontinued, and her drug regimen was composed mainly of piracetam and levetiracetam), alleviating her symptoms to an extent sufficient to allow recovery in a nursing home, with minimal

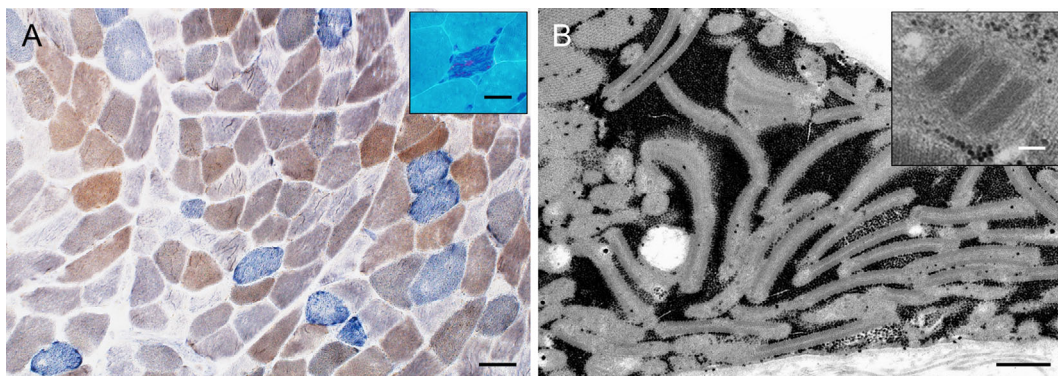


Figure 3. A histological examination of a muscle biopsy. (A) Double staining for succinate dehydrogenase (SDH) (blue) and cytochrome c oxidase (COX) (brown). COX-SDH staining shows COX-deficient fibers in 5% of the myofibers. Strongly stained SDH-reactive blood vessels are not observed. Scale bar: 50 μ m. Inset shows a ragged-red fiber on modified Gomori trichrome staining (Scale bar: 20 μ m). (B) Ultrastructural images showing marked subsarcolemmal proliferation of elongated mitochondria. Scale bar: 10 μ m. Inset shows paracrystalline inclusions (Scale bar: 100 nm).

support.

The MERRF-associated variant found in this patient occurred in a crucial position within the cloverleaf tRNA structure: at the base of the amino acid acceptor stem, juxtaposed to the nucleotide connecting the acceptor stem and D stem (Fig. 5). Variants of this type are more pathogenic than polymorphic mitochondrial tRNA variants (11). The mitochondrial tRNA informatics predictor suggests that the variant identified in our study is pathogenic (12). Furthermore, the patient's laboratory and histological findings (e.g. focal COX deficiency, subsarcolemmal accumulations of abnormally elongated mitochondria, and relatively low respiratory chain complex IV activity) were consistent with MERRF. These observations suggest that the identified variant is a new member of the family of MERRF-associated variants.

Regarding the conventional concept of MERRF, various clinical features are explained by differences in heteroplasmy and the threshold in various organs. However, in a case of severe encephalomyopathy, a homoplasmic m.5814A>G variant in tRNA^{Cys} has been reported (5). More recently, in a MERRF-like case, the homoplasmic m.15923A>G variant in tRNA^{Thr} was confirmed to be pathogenic using a detailed functional analysis (13). However, as in our case, the

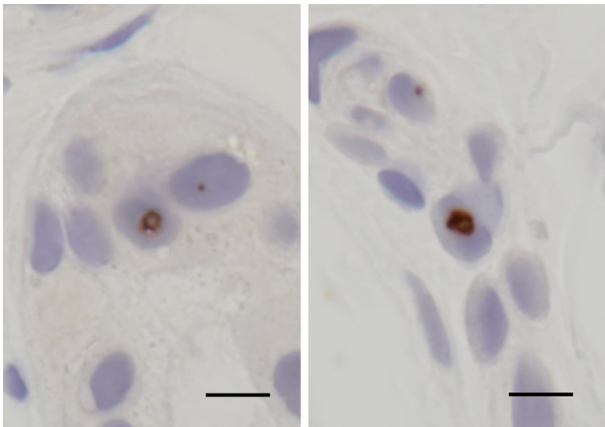


Figure 4. A histological examination of a skin biopsy. Anti-p62 antibody-positive intranuclear inclusions are observed in sweat glands. Scale bar: 10 μ m.

Table 2. Mitochondrial DNA Variants in the Patient.

bp	Variant	Reference	Gene product
73	G	A	D-loop
146	C	T	
263	G	A	
310	CTC	T	12S rRNA
489	C	T	
750	G	A	
856	G	A	16S rRNA
1,438	G	A	
2,706	G	A	
2,766	T	C	NADH dehydrogenase subunit 2
3,010	A	G	
4,769	G	A	
4,883	T	C	tRNA cysteine
5,178	A	C	
5,820	A	C	
7,028	T	C	Cytochrome c oxidase subunit I
8,414	T	C	ATP synthase F0 subunit 8
8,701	G	A	ATP synthase F0 subunit 6
8,860	G	A	Cytochrome c oxidase subunit III
9,540	C	T	
10,398	G	A	
10,400	T	C	NADH dehydrogenase subunit 3
10,873	C	T	NADH dehydrogenase subunit 4
11,719	A	G	
12,705	T	C	
14,668	T	C	NADH dehydrogenase subunit 5
14,692	G	A	NADH dehydrogenase subunit 6
14,766	T	C	tRNA glutamic acid
14,783	C	T	Cytochrome b
15,043	A	G	tRNA threonine
15,301	A	G	
15,326	G	A	
15,924	G	A	D-loop
16,223	T	C	
16,224	C	T	
16,245	T	C	D-loop
16,292	T	C	
16,362	C	T	
16,519	C	T	

Table 3. Enzymatic Activities of the Mitochondrial Respiratory Complexes.

#	Activity/complex II activity			Activity/CS activity		
	Patient	Control	%	Patient	Control	%
I	0.384	0.38±0.12 (0.16-0.52)	102	1.56	1.2±0.37 (0.44-1.8)	128
II				4.08	3.3±0.70 (2.6-4.8)	123
III	0.217	0.34±0.15 (0.12-0.62)	65	0.885	1.1±0.39 (0.55-1.8)	84
IV	0.648	1.2±0.20 (1.0-1.5)	55	2.64	3.8±0.45 (3.1-4.6)	69
V	0.317	0.26±0.13 (0.10-0.52)	124	1.29	0.85±0.47 (0.25-1.8)	152

The control values are obtained from six healthy individuals and are presented as mean±SD (range). Patient activity relative to control activity is shown as percentages (%). CS: citrate synthase, SD: standard deviation

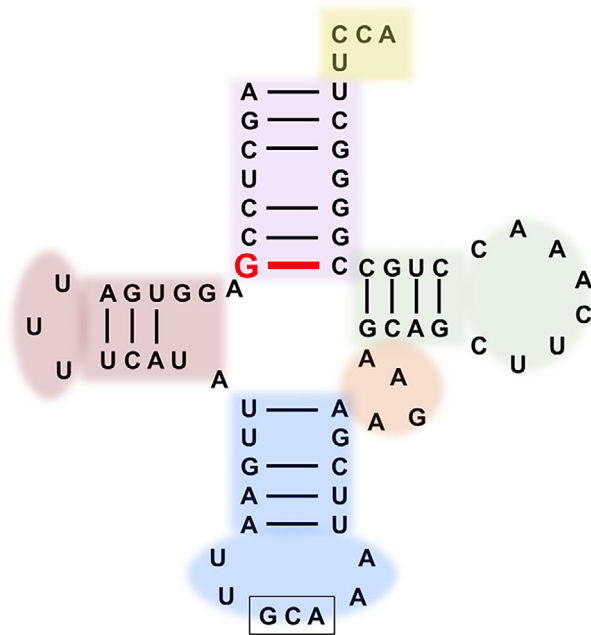


Figure 5. Cloverleaf structure of the human mitochondrial cysteine transfer RNA. The amino acid acceptor stem (purple), D-loop (brown), anticodon-stem (blue), variable region (orange), and T-loop (green) are shown. The position of the newly identified m.5820 variant is highlighted in red (shown as a sense strand of G complementary to C). This variant can disrupt the hydrogen bonds in the amino acid acceptor stem; it is predicted to be a possible pathogenic variant based on an *in silico* damage analysis by MitoTIP.

involvement of modifying nuclear genes could not be excluded, affecting the proportion of variant mtDNA or steady-state levels of mitochondrial tRNA.

To our knowledge, although abnormal mitochondrial inclusions were observed in a case of neuronal intranuclear inclusion disease (14), there has been no report of intranuclear inclusions in mitochondrial diseases. p62-positive intranuclear inclusions are usually observed in triplet-repeat disorders. In our investigation, we found no genetic evidence of such disorders or other diseases related to nuclear gene mutations in this patient. In FXTAS, expanded CGG repeats (FMRpolyG) affect mitochondria by reducing adenosine triphosphate (ATP) levels, mitochondrial transmembrane potential, mitochondrial supercomplex assemblies and activities, and the expression of mitochondrial DNA-encoded transcripts (15), as well as by altering the translocation of mitochondrial microRNAs (16). In addition, the association between the development of FXTAS among *FMR1* pre-mutation carriers (55 to 200 CGG repeats) and higher rates of mitochondrial DNA variants is evident (17). Our unpublished data regarding FXTAS (manuscript under preparation) and neuronal intranuclear inclusion disease (18) confirmed the presence of p62-positive intranuclear inclusions through a skin biopsy. This evidence indicates that the presence of intranuclear inclusions on a skin biopsy may be related to mitochondrial dysfunction. Although we were unable to find

any genetic evidence of nuclear gene involvement in our case, an unidentified nuclear gene may have existed as a modifier of the m.5820 variant. Finally, the connection between the intranuclear inclusions and the newly identified MERRF-associated variant is currently unclear and should be investigated thoroughly; we hope this case, despite its preliminary results, will serve as a basis for future studies.

All clinical information and samples were obtained for diagnostic purposes, and their scientific use was permitted through written informed consent.

The authors state that they have no Conflict of Interest (COI).

Financial Support

This work was supported by Research on Rare and Intractable Diseases from the Ministry of Health, Labour and Welfare (MHLW), Japan (Y. Goto); the Initiative on Rare and Undiagnosed Diseases by the Japan Agency for Medical Research and Development [grant numbers JP20ek0109486, JP20dm0107090, JP20ek0109301, JP20ek0109348, and JP20kk0205012 (N. Matsumoto)]; JSPS KAKENHI [grant numbers JP20K08164 (T. Mizuguchi) and JP17H01539 (N. Matsumoto)]; and intramural research grants for Neurological and Psychiatric Disorders of NCNP from the MHLW [grant numbers 30-7 (N. Matsumoto, Y. Goto), and 2-5 and 29-4 (I. Nishino)].

Acknowledgement

The authors thank Mina Hiraishi of the Tokyo Metropolitan Neurological Hospital for her excellent technical assistance.

References

- Velez-Bartolomei F, Lee C, Enns G. MERRF. GeneReviews® [Internet]. [cited 2021 Jun 22]. Available from: <https://www.ncbi.nlm.nih.gov/books/NBK1520/>
- Manfredi G, Schon EA, Bonilla E, Moraes CT, Shanske S, DiMauro S. Identification of a mutation in the mitochondrial tRNA^{Cys} gene associated with mitochondrial encephalopathy. *Hum Mutat* 7: 158-163, 1996.
- Santorelli FM, Siciliano G, Casali C, et al. Mitochondrial tRNA^{Cys} gene mutation (A5814G): a second family with mitochondrial encephalopathy. *Neuromuscul Disord* 7: 156-159, 1997.
- Karadimas C, Tanji K, Geremek M, et al. A5814G mutation in mitochondrial DNA can cause mitochondrial myopathy and cardiomyopathy. *J Child Neurol* 16: 531-533, 2001.
- Scuderi C, Borgione E, Musumeci S, et al. Severe encephalomyopathy in a patient with homoplasmic A5814G point mutation in mitochondrial tRNA^{Cys} gene. *Neuromuscul Disord* 17: 258-261, 2007.
- Wechsler D. Wechsler Adult Intelligence Scale - Fourth Edition (WAIS-IV). Pearson, San Antonio, TX, 2008.
- Matsunaga T, Kumanomido H, Shiroma M, Goto Y, Usami S. Audiological features and mitochondrial DNA sequence in a large family carrying mitochondrial A1555G mutation without use of aminoglycoside. *Ann Otol Rhinol Laryngol* 114: 153-160, 2005.
- MITOMAP. A human mitochondrial genome database [Internet]. [cited 2021 Jun 22]. Available from: <http://www.mitomap.org>
- Shimazaki H, Takiyama Y, Ishiura H, et al. A homozygous mutation of *C12orf65* causes spastic paraplegia with optic atrophy and neuropathy (SPG55). *J Med Genet* 49: 777-784, 2012.
- Morava E, Rodenburg RJ, Hol F, et al. Clinical and biochemical

- characteristics in patients with a high mutant load of the mitochondrial T8993G/C mutations. *Am J Med Genet A* **140**: 863-868, 2006.
11. Florentz C, Sissler M. Disease-related versus polymorphic mutations in human mitochondrial tRNAs. Where is the difference? *EMBO Rep* **2**: 481-486, 2001.
 12. Sonney S, Leipzig J, Lott MT, et al. Predicting the pathogenicity of novel variants in mitochondrial tRNA with MitoTIP. *PLoS Comput Biol* **13**: e1005867-e1005874, 2017.
 13. Lin H, Miyauchi K, Harada T, et al. CO₂-sensitive tRNA modification associated with human mitochondrial disease. *Nat Commun* **9**: 1875-1891, 2018.
 14. Morimoto S, Hatsuta H, Komiya T, Kanemaru K, Tokumaru AM, Murayama S. Simultaneous skin-nerve-muscle biopsy and abnormal mitochondrial inclusions in intranuclear hyaline inclusion body disease. *J Neurol Sci* **372**: 447-449, 2017.
 15. Gohel D, Sripada L, Prajapati P, et al. FMRpolyG alters mitochondrial transcripts level and respiratory chain complex assembly in Fragile X associated tremor/ataxia syndrome [FXTAS]. *Biochim Biophys Acta Mol Basis Dis* **1865**: 1379-1388, 2019.
 16. Gohel D, Sripada L, Prajapati P, et al. Expression of expanded FMR1-CGG repeats alters mitochondrial miRNAs and modulates mitochondrial functions and cell death in cellular model of FXTAS. *Free Radic Biol Med* **165**: 100-110, 2021.
 17. Alvarez-Mora MI, Santos C, Carreño-Gago L, et al. Role of mitochondrial DNA variants in the development of fragile X-associated tremor/ataxia syndrome. *Mitochondrion* **52**: 157-162, 2020.
 18. Sone J, Tanaka F, Koike H, et al. Skin biopsy is useful for the antemortem diagnosis of neuronal intranuclear inclusion disease. *Neurology* **76**: 1372-1376, 2011.

The Internal Medicine is an Open Access journal distributed under the Creative Commons Attribution-NonCommercial-NoDerivatives 4.0 International License. To view the details of this license, please visit (<https://creativecommons.org/licenses/by-nc-nd/4.0/>).